www.nature.com/leu Leukemia

### ARTICLE OPEN



LYMPHOMA

# Combining MCL-1 inhibition and CD37-directed chimeric antigen receptor T cells as an effective strategy to target T-cell lymphoma

Tayla B. Heavican-Foral 10 1,2,3, Felix Korell 10 4, Irene Scarfò 4,6, Caroline R. M. Wiggers 10 1,3, Allen Thayakumar B 10 1,2, Zachary Eisenbies 1, Foster Powers 10 2, Justin Hegel 10 1, Jianlin Liu 1,5, Steffen Kulp 10 2, Harrison Silva 10 4, Gongwei Wu 10 2,3, Anthony Letai 10 2,3, Kimberly Stegmaier 10 1,3, Jens G. Lohr 10 2,3,5, David M. Weinstock 10 2,3,7, Marcela V. Maus 10 3,4,8 2 and Birgit Knoechel 10 1,3,5,8 2

© The Author(s) 2025

Chimeric antigen receptor (CAR) T cell therapy has not yet been realized for T-cell lymphomas (TCL), partially due to challenges in identifying tumor-specific antigens. We previously reported selective expression of CD37 on malignant T cells in a subset of TCL. Herein, we demonstrate CAR-37 T cells specifically target CD37-positive TCL in part by activating the intrinsic apoptotic pathway. To maximize therapeutic index, we identified selective/targetable BH3 dependences in individual TCL models and combined with CAR-37 T cells. We show that BH3 mimetics do not alter CD37 antigen binding capacity on TCL and have minimal effects on CAR-37 T-cell phenotype or function. In TCL models with dependence on MCL-1, combining CAR-37 T cells and the MCL-1 inhibitor AZD5991 increases anti-TCL response and prolongs survival of xenografted mice. These findings suggest that personalized selection of BH3 mimetic/CAR-T combinations could maximize the therapeutic index for patients with TCL and possibly other diseases.

Leukemia (2025) 39:2452-2464; https://doi.org/10.1038/s41375-025-02697-1

### INTRODUCTION

T-cell lymphomas (TCLs) are a rare and heterogeneous group of neoplasms accounting for 10-15% of all non-Hodgkin lymphomas [1]. The World Health Organizations recognizes over 30 subtypes, with most associated with poor prognosis [1, 2]. Frontline therapy for patients is often a combination chemotherapy regimen, yet a large fraction of patients will never reach remission or will experience relapse [3, 4]. Clinical trials for patients with relapsed/refractory TCL have indicated brief responses to multiple agents including histone deacetylases inhibitors, pralatrexate, and bortezomib [3, 5–7]; therefore, limited improvements in overall survival have been achieved. Thus, there is an unmet need to generate novel therapeutic strategies for patients with TCL.

Chimeric antigen receptor (CAR) T cell therapy has been successful against B-cell malignancies by targeting CD19 [8, 9]. However, the generation of CAR T cells targeting TCL has been challenging since many surface proteins expressed on malignant TCL cells are also present on nonmalignant T cells which could result in severe immunodeficiency or fratricide [10]. CAR T cells targeting CD3, CD5, CD7, T-cell receptor  $\beta$ , and antigens with restricted expression are being investigated; however, targeting these surface antigens may require transient CAR expression or

gene editing to reduce on-target, off-tumor effects [10–16]. Further, expression of these molecules is often lost in TCL [17, 18]. Recently, we identified CD37 as a target for CAR T cells in TCL that spares nonmalignant T cells [19]. CD37 is a transmembrane protein of the tetraspanin superfamily and expressed most abundantly on mature B cells. The expression of CD37 on malignant T cells distinguishes it from other CAR T-cell targets under development against TCL. These findings support anti-CD37 (CAR-37) CAR T cells as a promising immunotherapy against TCL warranting further investigation.

Evading apoptosis is a hallmark of tumor cell survival. We recently reported that anti-apoptotic BCL-2 family members are necessary for TCL apoptotic escape and therefore are selective and targetable vulnerabilities [20]. To assess functional dependence, BH3 profiling was performed and high concordance between predicted BH3 dependences and sensitivity to BH3 mimetics (i.e., ABT199 [BCL-2 inhibitor] [21], ABT263 [BCL-2/BCL-xL inhibitor] [22], and AZD5991 [MCL-1 inhibitor] [23]) was observed [24, 25], demonstrating that BH3 profiling can accurately identify targetable anti-apoptotic dependences in TCL [20, 26]. Recently, it has been reported that BH3 mimetics augment CAR-19 T cell and natural killer (NK) cell-based immunotherapy by targeting

<sup>1</sup>Pediatric Oncology, Dana-Farber Cancer Institute, Boston, MA, USA. <sup>2</sup>Medical Oncology, Dana-Farber Cancer Institute, Boston, MA, USA. <sup>3</sup>Harvard Medical School, Boston, MA, USA. <sup>4</sup>Cancer Center, Massachusetts General Hospital, Boston, MA, USA. <sup>5</sup>Huntsman Cancer Institute, Salt Lake City, UT, USA. <sup>6</sup>Present address: ArsenalBio, South San Francisco, CA, USA. <sup>7</sup>Present address: Merck Research Laboratories, Boston, MA, USA. <sup>8</sup>These authors contributed equally: Marcela V. Maus, Birgit Knoechel.

 $^{oxtimes}$ email: mvmaus@mgh.harvard.edu; birgit\_knoechel@dfci.harvard.edu; birgit.knoechel@hci.utah.edu

Received: 8 October 2024 Revised: 29 May 2025 Accepted: 7 July 2025 Published online: 30 July 2025

mitochondrial apoptosis [27–29]. These findings are crucial as 20-60% of patients with B-cell malignancies treated with CAR-19 T cells eventually relapse [30, 31]. Thus, a central issue in the field is ways to potentiate CAR T-cell activity while maintaining tolerability, meriting the investigation of BH3 mimetics to enhance CAR-37 antitumor activity against TCL.

### METHODS Cell lines

DL-40 and MTA were purchased from the Japanese Collection of Research Biosources Cell Bank. FEPD was kindly provided by Leandro Cerchietti (Weill Cornell Medicine, New York, USA as approved by the Ontario Cancer Institute. HUT78 was purchased from American Type Culture Collection. SMZ1 was kindly provided by Hitoshi Ohno (Tenri Medical Institute, Tenri, Japan). Cell lines were routinely tested for mycoplasma using a PCR-based approach (SigmaAldrich—GeM Mycoplasma Detection Kit), and authenticity was validated by short tandem repeat (STR) profiling at the Molecular Diagnostics Laboratory at Dana-Farber Cancer Institute. Cell lines were given a minimum of 1-week after thaw to recover before experimental use.

### **CAR T-cell constructs**

CAR T-cell constructs were designed, one each targeting CD19 (CAR-19) and CD37 (CAR-37) antigens. Both constructs were synthesized and cloned into a second-generation lentiviral plasmid backbone under the regulation of a human EF-1 $\alpha$  promoter, and they each contain a CD8 hinge, 4-1BB costimulatory domain, and CD3 $\zeta$  signaling domain. A truncated EGFR reporter was included to facilitate enumeration of transduction efficiency (Fig. S1).

### **BH3** mimetics

ABT199 (#HY-15531) and ABT263 (#HY-10087) were purchased from MedChemExpress. AZD5991 was provided by AstraZeneca. Dry solid drugs were dissolved in DMSO to 10 mM stock solutions for in vitro experiments. For in vivo experiments, AZD5991 was formulated in 30% hydroxy-propylbeta-cyclodextrin (Sigma Aldrich, #332607) in water-for-injection adjusted to pH 9.0–9.5 using 1 M Meglumine (Santa Cruz Biotechnology, #SC-205383B) to a concentration of 10 mg/mL.

Additional methods are included in Supplementary Information.

### **RESULTS**

### CAR-37 T cells demonstrate activity against subtypes of TCL

CD37 surface expression on TCL-derived cell lines and a patient-derived xenograft (PDX) DFTL-28776 [19] was confirmed (Figs. 1A, S2A). To demonstrate in vitro efficacy, we performed a luminescence-based cytotoxicity assay and observed that increasing concentrations of CAR-37 T cells led to specific killing of TCL lines, whereas minimal or no killing was observed in the control CAR-19 and untransduced (UTD) T cell groups (Figs. 1B, S2B).

To evaluate the in vivo antitumor activity of CAR-37 T cells, mice were injected with luciferase-expressing SMZ1 + CD37 cells (Fig. 1C). Tumor burden was assessed by bioluminescence imaging (BLI), and CAR-37, CAR-19, or UTD T cells were administered. Within 7 days there was significant (p < 0.01) reduction in tumor burden in the CAR-37 T-cell treated animals. No disease was detected at day 14 and persisted through the 80-day evaluation period (Fig. 1D). Similarly, mice were injected with luciferase-expressing HUT78 cells (Fig. S2C), which has >35-fold lower antigen binding capacity of CD37 compared to SMZ1 + CD37. The mice were treated at a later timepoint (7.21E + 07 total flux compared to 6.76E + 06 in the SMZ1 + CD37 cohort) yet achieved inhibition of tumor growth seven days post CAR-37 T cells (Fig. S2D).

We also tested CAR-37 T cells against PDX DFTL-28776 in vivo. After confirming disease engraftment, CAR-37, CAR-19, or UTD T cells were administered (Fig. 1E). At day seven, a rapid and significant (p < 0.001) decrease in tumor burden was observed in CAR-37 T-cell cohort. However, at day 28 we observed tumor

recurrence with progression through the 90-day collection timepoint, albeit at a slower rate compared to the control groups in which all animals were moribund by day 35 (Figs. 1F, S2E).

To investigate disease progression after CAR-37 treatment, liver cells harvested from CAR-37 treated animals in Fig. 1F were injected and treated with CAR-37 or UTD T cells (Fig. 1G). By day six, a rapid and significant (p < 0.001) decrease in disease was observed in animals (re)treated with CAR-37 T cells and remained stable until day 35. On day 42, another dose of CAR-37 T cells was administered, resulting in stable disease for 30 days in all animals except for one which progressed. At day 70, progression continued in a subset of animals, yet survival was prolonged in some animals >100 days, and two remained tumor-free per BLI through the 140-day evaluation period (Fig. 1H). Thus, TCL PDX cells can undergo multiple rounds of disease response and progression after in vivo exposure to CAR-37 T cells, which may eradicate disease in some animals.

To further assess the degree of response, bone marrow, liver, and spleen were harvested from animals in Fig. 1G/H. We detected significantly (p < 0.001) less disease in the bone marrow of animals treated with CAR-37 (Fig. 1I). Importantly, CD37 antigen remained present on the tumor cells and no differences in antigen binding capacity between treatments were observed (Fig. 1J). We evaluated the same compartments for non-tumor T-cells. A range of 0-7% was measured in all compartments, except for one no/low tumor burden animal with 15% non-tumor T cells persisting in the spleen (Fig. 1K). Of the non-tumor T cells in the CAR-37 T cell treated animals, more than 90% were CAR-positive (Fig. 1L). Together, these results indicate that CAR-37 T cells actively target TCLs both in vitro and in vivo, and that recurrent disease was susceptible to repeated treatment with CAR-37 T cells.

### CAR-37 T cells induce apoptosis in TCL

One way T cells kill target cells is by secreting granzymes and perforin to trigger the mitochondria-mediated intrinsic apoptotic pathway [32–34]. When cocultured, CAR-37 T cells led to significant externalization of phosphatidylserine on target cells (Fig. 2A/B) and caspase-3 activation (Fig. 2C/D) in a dose-dependent manner, signifying induction of apoptosis. Similarly, CAR-37 T cells resulted in significant loss of active mitochondrial membrane potential in target cells (Fig. 2E/F), consistent with mitochondrial apoptosis.

To further explore apoptosis induced by the CAR-37 T cells, we performed BH3 profiling to measure mitochondrial apoptotic priming via cytochrome c release [24, 25]. Target lines were BH3 profiled after coculture with CAR-37 T cells. As shown in Fig. 2G and quantified in 2H, CAR-37 T cells alone induced rapid and significant cytochrome c release ( $p \le 0.001$ ) measured by exposure to DMSO. To define the specificity of apoptosis induction, we performed BH3 profiling on the TCL lines after coculture with UTD, CAR-19, and CAR-37 T cells. A modest increase in apoptotic priming was observed with UTD and CAR-19 T cells upon DMSO exposure and even greater with exposure to BIM, a promiscuous pro-apoptotic activator (Fig. S3), suggesting that allogeneic T cells may nonspecifically lower a tumor cell's apoptotic threshold. Taken together, our results indicate that CAR T-cell treatment induces mitochondrial apoptosis in a dose-escalating manner, which may be further potentiated in combination with apoptosisinducing agents.

### BH3 mimetics do not change the immunophenotype and subset distribution of CAR-37 T cells in vitro

To evaluate the feasibility of combining BH3 mimetics and CAR T cells, we determined the impact of BH3 mimetics on CAR-37 T cell phenotypes. We performed BH3 profiling on CAR-37 T cells stimulated with interleukin 2 (IL-2) or target FEPD cells. General priming was measured in response to BIM (Fig. 3A) and showed

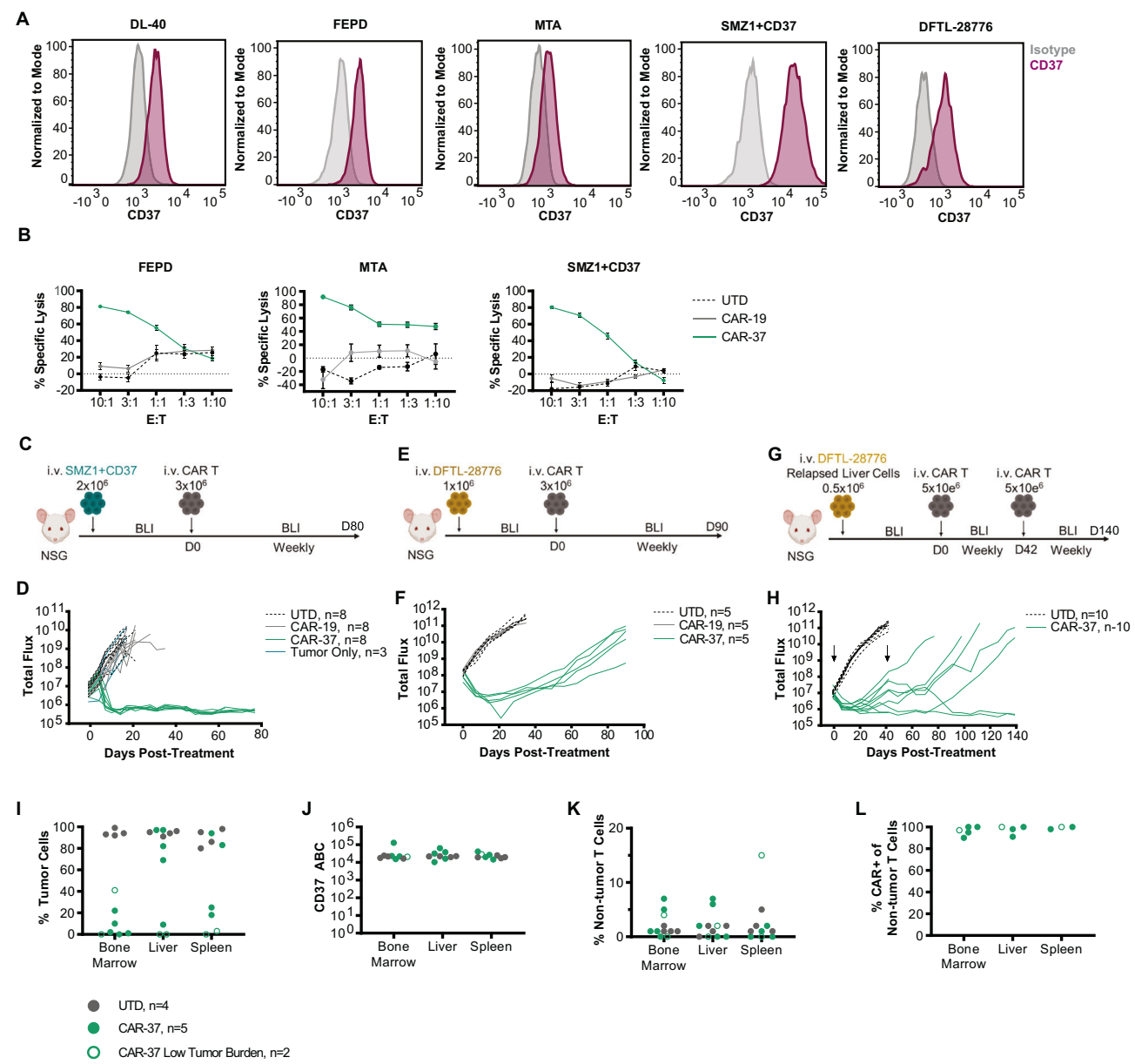


Fig. 1 CAR-37 T cells demonstrate antitumor activity against T-cell lymphomas. A Fluorescence-activated cell sorter (FACS) histograms of TCL cell lines and a patient-derived xenograft line stained with CD37 and isotype control. DL-40: ALK- anaplastic large cell lymphoma cell line, FEPD: ALK- anaplastic large cell lymphoma cell line, MTA: natural killer (NK)/T-cell lymphoma cell line, SMZ1 + CD37: peripheral TCL-not otherwise specified cell line transduced with CD37, and DFTL- 28776: a T prolymphocytic leukemia patient-derived xenograft line. B Cytotoxic capacity of CAR-37 T cells was measured after overnight (16-hour) coculture with target TCL cell lines. CAR T cells were cocultured at the indicated effector to target (E:T) cell ratios with the designated tumor cell line. Increasing concentrations of CAR-37 T cells led to specific killing, whereas no or minimal killing was observed in the control groups (untransduced [UTD] and CAR-19 T cells). Performed with 3 donors. Mean  $\pm$  SEM shown. C Experiment schematic: NSG mice were injected intravenously with  $2 \times 10^6$  SMZ1 + CD37 (CBG-GFP) cells and monitored by weekly bioluminescence imaging (BLI) for tumor burden. At day 0, mice were randomly assigned based on tumor burden to receive  $3 \times 10^6$ UTD, CAR-19, or CAR-37 T cells or nothing (tumor only). D The total flux (photons/seconds) of mice in the 4 treatment cohorts at weekly intervals. Monitoring stopped at day 80. UTD, CAR-19, and CAR-37; n = 8. Tumor only; n = 3. **E** Experiment schematic: NSG mice were injected intravenously with  $1\times10^6$  DFTL-28776 cells and monitored by weekly BLI for tumor burden. At day 0, mice were randomly assigned based on tumor burden to receive 3 × 10<sup>6</sup> UTD, CAR-19, or CAR-37 T cells. **F** The total flux (photons/seconds) of mice in the 3 treatment cohorts at weekly intervals. Monitoring stopped at day 90. UTD, CAR-19, CAR-37; n = 5. **G** Experiment schematic: NSG mice were injected intravenously with  $0.5 \times 10^6$  relapsed liver tumor cells from DFTL-28776 mice treated with CAR-37 T cells in (**E, F**) and monitored by weekly BLI for tumor burden. At day 0, mice were randomly assigned based on tumor burden to receive  $5 \times 10^6$  UTD or CAR-37 T cells. At day 42, another  $5 \times 10^6$ CAR-37 T cells were administered. H The total flux (photons/seconds) of mice in the 2 treatment cohorts at weekly intervals. Monitoring stopped at day 140. UTD and CAR-37; n = 10. Flow cytometry was performed on cells harvested from the bone marrow, liver, and spleen of mice in panels G/H with sufficient material. I Percent of DFTL-28776 tumor cells (CD45+, CD3-). J CD37 antigen binding capacity (ABC) on the surface of DFTL-28776 tumor cells. K Percent of non-tumor T cells (CD45+, CD3+). L Percent of non-tumor T cells expressing the CAR construct (CD45+, CD3+, tEGFR+) in mice treated with CAR-37 T cells.

**SPRINGER NATURE**Leukemia (2025) 39:2452 – 2464

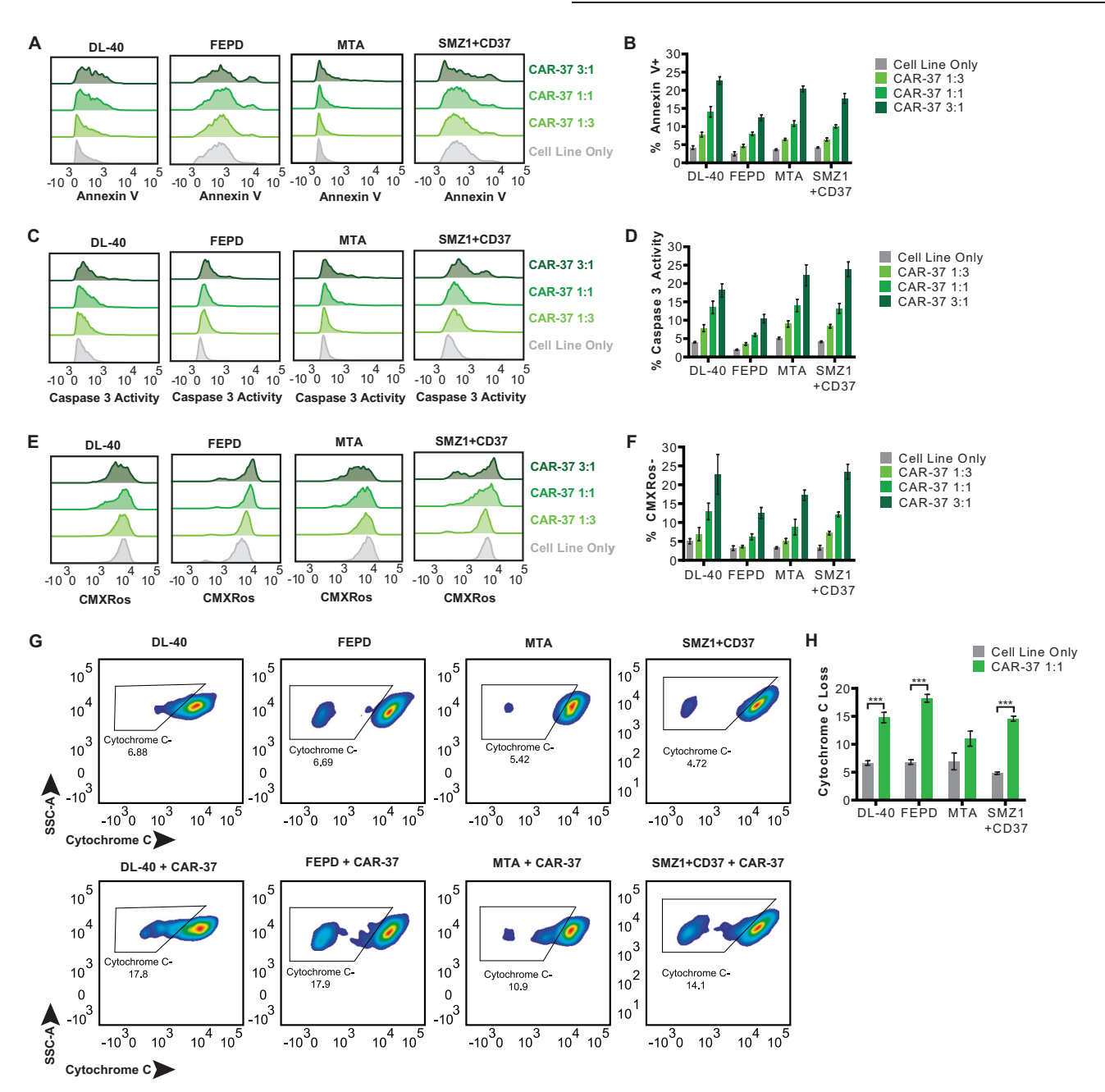
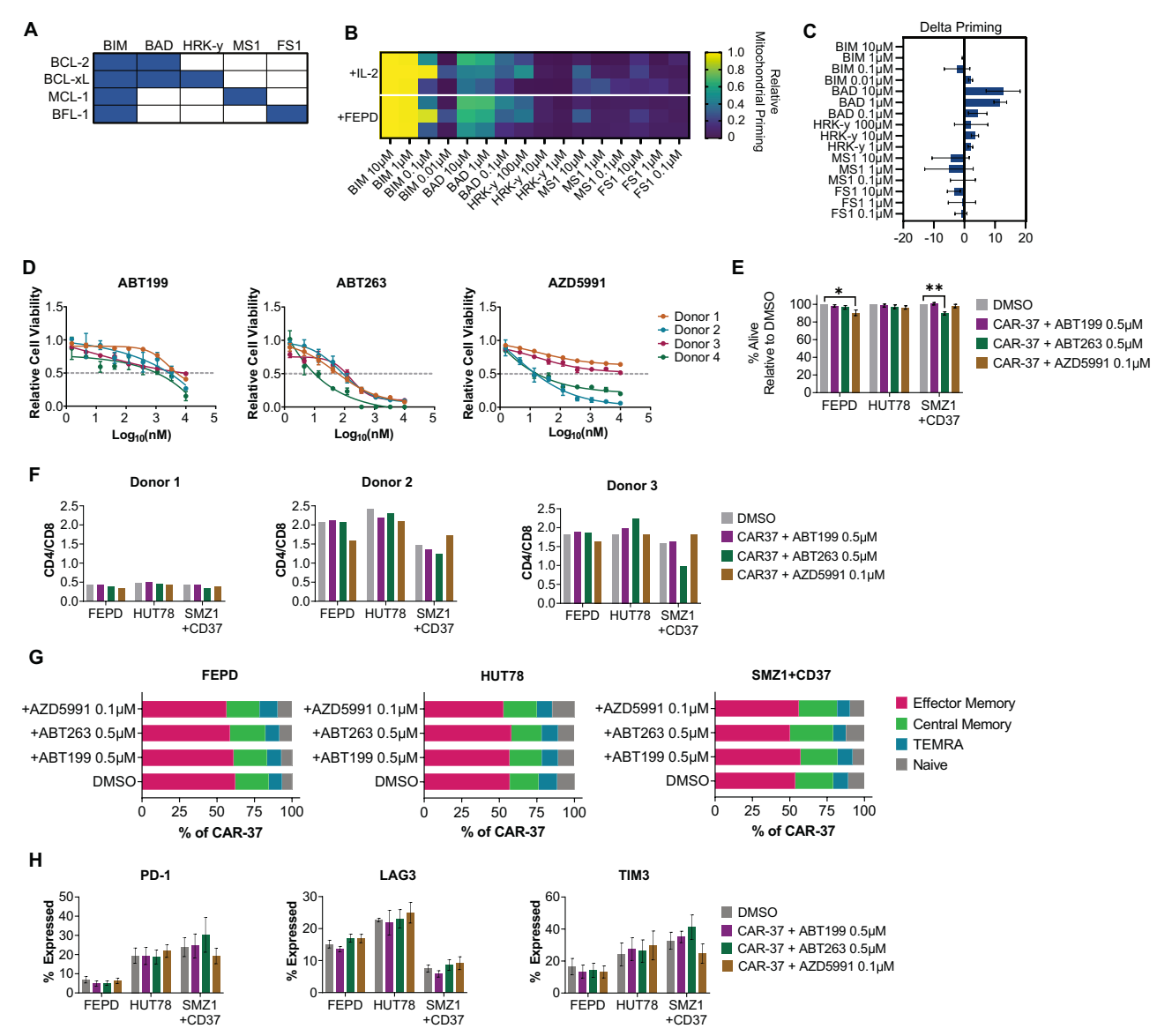


Fig. 2 CAR-37 T cells induce mitochondrial apoptosis in T-cell lymphoma cells. A Representative FACS histograms demonstrating exposure of phosphatidylserine on TCL target cells after 5-hour CAR-37 T-cell treatment at 3 effector to target (E:T) cell ratios, measured by annexin V staining. B Bar plot representation of panel A performed with 3 donors. Mean  $\pm$  SEM shown. C Representative FACS histograms demonstrating activation of caspase-3 in TCL target cells after 5-hour CAR-37 T-cell treatment at 3 E:T cell ratios, measured by BioTracker NucView 405 Blue Caspase-3 Dye. D Bar plot representation of (C) performed with 3 donors. Mean  $\pm$  SEM shown. E Representative FACS histograms demonstrating loss of mitochondrial membrane potential (CMXRos-) in TCL target cells after 5-hour CAR-37 T-cell treatment at 3 E:T cell ratios, measured by MitoTracker Red CMXRos Dye. F Bar plot representation of (E) performed with 3 donors. Mean  $\pm$  SEM shown. G Representative FACS plots demonstrating increased cytochrome c release from the mitochondria of TCL target cells upon 4-hour CAR-37 T-cell treatment at a 1:1 E:T cell ratio (bottom). Cytochrome c release was measured by BH3 profiling. DMSO was used instead of BH3 peptides. H Bar plot representation of (G) performed with 3 donors. Mean  $\pm$  SEM shown. \*\*\*\* $p \le 0.001$  \*\*\* $p \le 0.05$ , Student's t-test.

no difference between the two stimulation conditions (Fig. 3B). Evaluation of the specific peptides revealed increased cytochrome c release in response to BAD and HRK-y, which suggested a BCL-xL dependence that was further augmented upon coculture with target cells. Conversely, responses to MS1 and FS1 decreased or were unchanged (Fig. 3B/C). Next, we exposed IL-2 stimulated CAR-37 T cells derived from four healthy donors to BH3 mimetics ABT199 targeting BCL-2 [21], ABT263 targeting BCL-2/BCL-xL [22], and AZD5991 targeting MCL-1 [23]. Overall, CAR T cells were most

sensitive to ABT263 (Fig. 3D). However, two donors were sensitive to AZD5991 whereas the other two maintained ≥50% viable at 10uM (Fig. 3D), highlighting variability between donors and the potential need to BH3 profile CAR T cells prior to combination with BH3 mimetics.

We then exposed CAR-37 T cells to target cells and BH3 mimetics simultaneously. Notably, these cell lines have varying levels of CD37 expression and BH3 dependences. At the concentrations effective for targeting TCL lines, minimal to



**Fig. 3 BH3 mimetics do not alter CAR-37 T cell phenotype. A** Key indicating the specificity of synthetic BH3 peptides used in BH3 profiling. **B** Heatmap of relative mitochondrial apoptotic priming of CAR-37 T cells stimulated with 40 ng/mL IL-2 (top) or the FEPD target cells at a 2:1 effector to target (E:T) cell ratio (bottom) for 24 h normalized to DMSO. Each tile represents the triplicate average of 1 of 3 donors. **C** Delta priming of CAR-37 T cells after 24 h stimulation with IL-2 or FEPD target cells. Positive values indicate increased mitochondrial apoptotic priming upon target cell (FEPD) stimulation. Delta priming was calculated as: priming<sub>stimulated FEPD</sub> – priming<sub>stimulated IL-2</sub>. Mean ± SEM from 3 donors shown. **D** Relative cell viability of CAR-37 T cells derived from 4 healthy donors with 48-hour ABT199, ABT263, or AZD5991 treatment over a range of concentrations measured by CellTiter-Glo. Mean ± SEM shown. **E** Bar plot representation of FACS data evaluating CAR-37 T cells lines at a 1:1 E:T cell ratio and DMSO, ABT199 (0.5 μM), or AZD5991 (0.1 μM), measured by DAPI. Mean ± SEM of 3 donors shown. \*\*\*\*\* $p \le 0.0001$ , \*\*\*\*\*  $p \le 0.001$  \*\*\*\* $p \le 0.01$ , \*\* $p \le 0.05$ , One-way ANOVA. **F** Bar plot representation of FACS data evaluating CD4 and CD8 subset distribution of CAR-37 T cells after a 48 h coculture with target TCL lines at a 1:1 E:T cell ratio and DMSO, ABT199 (0.5 μM), ABT263 (0.5 μM), or AZD5991 (0.1 μM). **G** Bar plot representation of CAR-37 T cell immunophenotypes after a 48-hour coculture with target TCL lines at a 1:1 E:T cell ratio and DMSO, ABT199 (0.5 μM), ABT263 (0.5 μM), or AZD5991 (0.1 μM). CCR7 and CD45RA surface expression were analyzed by FACS to classify the CAR T cells as effector memory (EM; CCR7+,CD45RA-), central memory (CM; CCR7+,CD45RA), naïve (CCR7+, CD45RA+), or effector memory T cells re-expressing CD45RA (TEMRA; CCR7-,CD45RA-). Mean of 3 donors shown. **H** Bar plot representation of FACS data evaluating surface expression of T-cell exhaustion markers PD-1, LAG3, a

no effect on CAR-37 T cell viability was observed between TCL lines or BH3 mimetics, yet the strongest effect was observed with SMZ1+CD37 and ABT263 with an 11% reduction in viability (Fig. 3E). Under similar conditions, we evaluated CD4 and CD8 subset distribution. Although CD4/CD8 ratios varied between healthy donors, we did not observe a consistent superior expansion of one population under a particular culture

condition. However, it appeared that CD4 cells were those effected in the FEPD/AZD5991 and SMZ1 + CD37/ABT263 conditions with decreased viability (Fig. 3F). Subsequently, CAR-37 T cells were immunophenotyped with no significant differences amongst coculture conditions detected. Approximately 60% had an effector memory phenotype, followed by ~20% with a central memory phenotype, and the remaining equally distributed

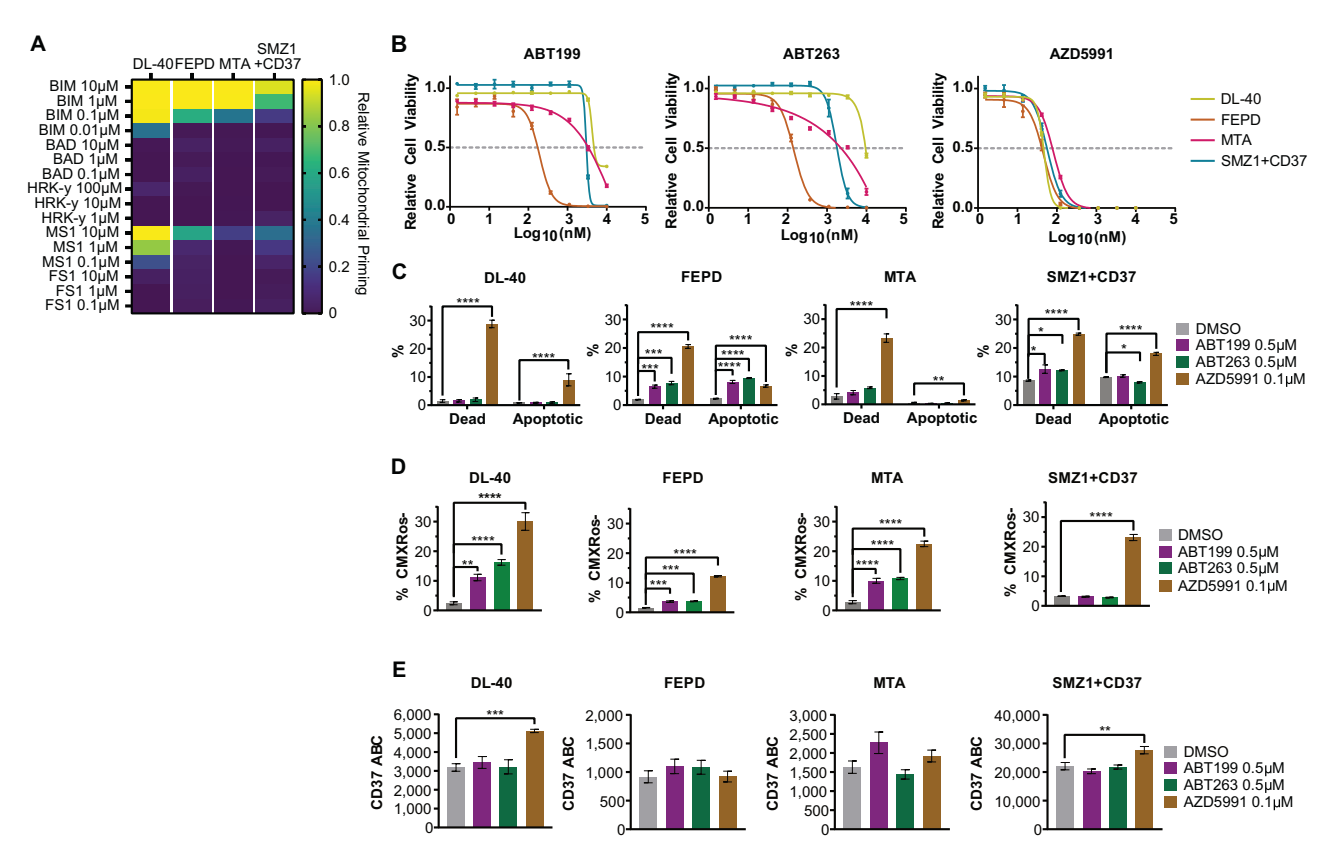


**Fig. 4 T-cell lymphomas are selectively dependent on pro-apoptotic proteins. A** Heatmap of the baseline mitochondrial apoptotic priming status normalized to DMSO of the TCL lines. Triplicate average shown. **B** Relative cell viability of TCL lines with 72 h ABT199, ABT263, or AZD5991 treatment over a range of concentrations measured by CellTiter-Glo. Mean ± SEM shown. **C** Bar plot representation of FACS data (Fig. S5) demonstrating induction of cell death and exposure of phosphatidylserine on the TCL lines after 24 h exposure to DMSO, ABT199 (0.5 μM), ABT263 (0.5 μM), or AZD5991 (0.1 μM), measured by DAPI and annexin V staining. Mean ± SEM shown. \*\*\*\* $p \le 0.0001$ , \*\*\* $p \le 0.001$  \*\*\* $p \le 0.005$ , One-way ANOVA. **D** Bar plot representation of FACS data demonstrating loss of mitochondrial membrane potential (CMXRos-) in the TCL lines after 24 h exposure to DMSO, ABT199 (0.5 μM), ABT263 (0.5 μM), or AZD5991 (0.1 μM), measured by MitoTracker Red CMXRos Dye. Mean ± SEM shown. \*\*\*\*\* $p \le 0.0001$ , \*\*\*\*\* $p \le 0.001$  \*\*\* $p \le 0.01$ , \*\* $p \le 0.05$ , One-way ANOVA. **E** Bar plot representation of FACS data showing CD37 antigen binding capacity (ABC) on the surface of the TCL lines after 24 h exposure to DMSO, ABT199 (0.5 μM), or AZD5991 (0.1 μM). Mean ± SEM shown. \*\*\*\*\* $p \le 0.0001$ , \*\*\*\* $p \le 0.0001$  \*\*\*\* $p \le 0.001$  \*\*\*\* $p \le 0.001$  \*\*\* $p \le 0.005$ , One-way ANOVA.

between effector memory T cells re-expressing CD45RA (TEMRA) and naive phenotypes (Fig. 3G). Additionally, we evaluated known T-cell activation/exhaustion markers (e.g., PD-1, TIM3, and LAG3) and differences were only observed in respect to the target line (Fig. 3H). Functional activity of CAR-37 T cells in the presence of BH3 mimetics was analyzed by measuring cytokine production from the coculture supernatants. Expectedly, elevated levels of interferon gamma (IFNy) and interleukin 13 (IL-13) were detected and likely resulted from 4-1BB activation [35, 36] (Fig. S4). Together, these results suggest a promising therapeutic opportunity for augmenting CAR-based therapies with BH3 mimetics given the minimal effects on activated CAR-37 T cells.

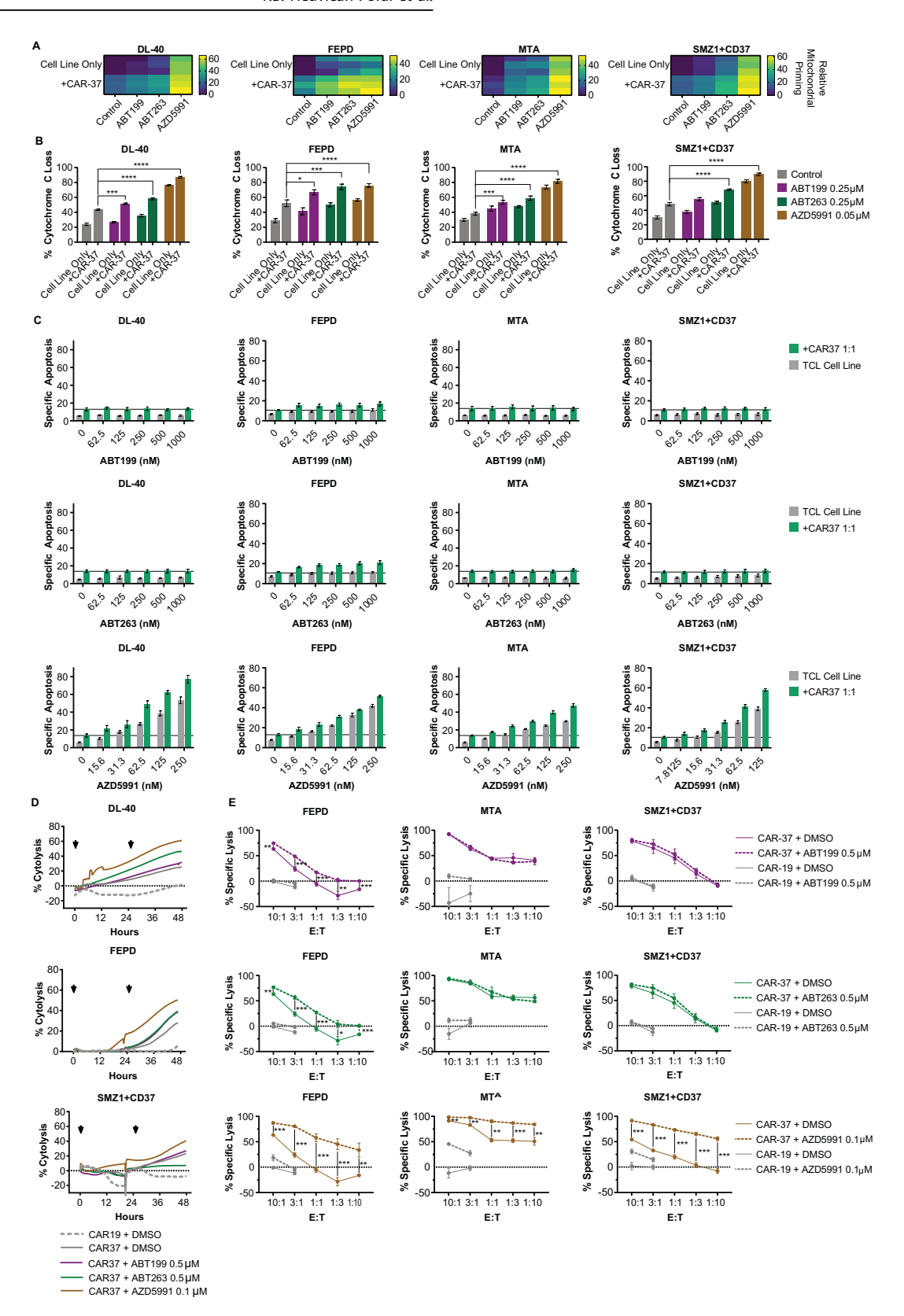
## BH3 mimetics selectively target pro-apoptotic proteins in TCL with no effect on CD37 antigen binding capacity

We hypothesized that BH3 mimetics targeting specific vulnerabilities in anti-apoptotic proteins can potentiate the tumoricidal activity of CAR-37 T cells by pushing TCL cells over their apoptotic threshold. We performed BH3 profiling on the TCL lines to predict their selective BH3 dependencies. Specificity in interaction of the BH3 domains of BH3-only proteins Bad, Bid, Bim, Hrk, Noxa, Puma, and BNip3 has been previously described [37–39]. Corresponding to previous reports [20], all TCL lines evaluated were MCL-1-dependent, indicated by cytochrome c release in response to MS1 (Fig. 4A).

Next, we exposed the lines to the BH3 mimetics, and all were most sensitive to AZD5991 which corresponded to their predicted MCL-1 dependence (Fig. 4B). Selectivity of the BH3 mimetics was further evaluated in the TCL lines by measuring specific apoptosis and mitochondrial membrane potential. As anticipated, AZD5991 treatment resulted in significant killing of the MCL-1-dependent lines (Fig. 4C). Similarly, significant loss of mitochondrial membrane potential was detected in the lines when exposed to AZD5991 (Fig. 4D). Importantly, and although not expected exposure to BH3 mimetics did not reduce CD37 antigen binding capacity on the surface of the lines, but rather increased it under some conditions (Fig. 4E). Collectively, these results demonstrate that BH3 profiling accurately predicts apoptotic dependences, which can be selectively targeted with BH3 mimetics without compromising target antigen binding capacity.

# Personalized BH3 mimetic combinations with CAR-37 T cells increase killing of TCL in vitro and in vivo

Since BH3 mimetics had minimal effects on CAR-37 T cells and selectively targeted TCL lines, we sought to test the combination in vitro. TCL lines were cocultured with BH3 mimetics or DMSO alone and in combination with CAR-37 T cells prior to BH3 profiling. The cocultured cells were exposed to BIM to measure overall apoptotic priming and we detected exposure to CAR-37



T cells increased priming under all coculture conditions (Fig. 5A). Yet, when comparing cytochrome c loss relative to exposure to CAR-37 T cells alone, CAR-37 T cells were most greatly augmented by the BH3 mimetic targeting the cell line's predicted BH3 dependence, AZD5991 (Fig. 5A/B).

Next, we measured specific apoptosis. As consistently observed, FEPD cell death increased with all three BH3 mimetics combined with CAR-37 T cells; however, to the highest extent with AZD5991. When evaluating DL-40, MTA, and SMZ1 + CD37, enhanced killing was only observed when CAR-37 T cells were combined with AZD5991 (Fig. 5C).

Fig. 5 BH3 mimetics potentiate the tumoricidal activity of CAR-37 T cells in vitro. A Delta priming of TCL lines after 2-hour treatment with DMSO, ABT199 (0.25 μM), ABT263 (0.25 μM), or AZD5991 (0.05 μM) in the presence or absence of CAR-37 T cells at a 1:1 effector to target (Ε:Τ) cell ratio, measured by cytochrome c release in response to BIM peptide exposure. BIM peptide concentration was 0.01 µM for DL40 and  $0.1 \, \mu M$  for FEPD, MTA, and SMZ1 + CD37. Delta priming was calculated as: priming treated - priming untreated (DMSO). Each tile represents the triplicate average of 1 of 3 donors. **B** Mitochondrial apoptotic priming status defined as the amount (0–100%) of cytochrome c release induced by BIM peptide in (A). Mean  $\pm$  SEM of 3 donors shown. \*\*\*\*  $p \le 0.0001$ , \*\*\*  $p \le 0.001$  \*\* $p \le 0.01$ , \* $p \le 0.05$ , Two-way ANOVA. C Specific apoptosis of target TCL lines treated with escalating doses of ABT199, ABT263, or AZD5991 in the presence or absence of CAR-37 T cells at a 1:1 E:T cell ratio for 4 h, measured by Annexin V. Cell lines in the presence of CAR-37 T cells were pre-exposed to the CAR T cells for 1 h prior to addition of the BH3 mimetics. Of note, reduced concentrations of AZD5991 compared to ABT199 and ABT263 were used to allow for differentiation of improved tumor killing since the TCL lines were highly sensitive to this inhibitor. The solid line indicates the threshold of CAR-37 T cell killing. Mean ± SEM of 3 donors shown. D TCL target cell lines were cultured with CAR-19 or CAR-37 T cells in combination with DMSO, ABT199 (0.5 µM), ABT263 (0.5 µM), or AZD5991 (0.1 µM) for 48 h. The BH3 mimetics were replenished every 24 h as indicated by the arrows. Real-time cytolysis was measured by an xCELLigence system (ACEA) and calculated as: % cytolysis = [(cell index of target cells - cell index of CAR-T cells) / (cell index of target cells)] × 100. Mean ± SEM of 3 donors shown. **E** Cytotoxic capacity of CAR-19 or CAR-37 T cells in combination with DMSO, ABT199 (0.5 µM), ABT263 (0.5 µM), or AZD5991 (0.1 µM) was measured after overnight coculture with target TCL lines. CAR T cells were cocultured at the indicated E:T cell ratios with the indicated tumor cell lines. Percent specific lysis was calculated as: ((target cell with drug only RLU – well of interest RLU) / target cell with drug only RLU) × 100. Mean  $\pm$  SEM of 3 donors shown. \*\*\*\*  $p \le 0.0001$ , \*\*\*  $p \le 0.001$  \*\*\*  $p \le 0.01$ , \* $p \le 0.05$ , Student's *t*-test.

Confirming our earlier results via a real-time cell analysis, CAR-37 T cell antitumor activity was enhanced when combined with AZD5991 (Fig. 5D). We observed dose-escalating CAR-37 T cell antitumor activity against the FEPD line with each BH3 mimetic. When evaluating MTA and SMZ1+CD37 lines, increased killing was only detected in combination with AZD5991 as expected (Fig. 5E). In response to the earlier observation that allogeneic T cells lowered a tumor cell's apoptotic threshold (Fig. S3), we measured mitochondrial apoptotic priming (BH3 profiling) and induction of apoptosis (Annexin V) in response to AZD5991 with untransduced, CAR-19, and CAR-37 T cells. A trend of increased susceptibility to non-specific allogenic T-cell killing was observed; however, the only combination that resulted in significantly greater tumor cell death in all four models tested was CAR-37 and AZD5991 (Fig. S6A-C). Therefore, these data suggest that directed T-cell killing is most optimal for targeting tumor cells alone and in combination with AZD5991. Together, these results demonstrate that apoptotic priming and cell death of the target tumor cells are significantly enhanced by combining CAR-37 T cells and BH3 mimetics.

To extend these findings in vivo, mice were injected with luciferase-expressing FEPD cells. Once engrafted, CAR-37 or CAR-19 T cells were administered. The next day, cohorts received either vehicle or AZD5991 for three weeks (Fig. 6A). Six days post-treatment initiation, we observed stable disease in all cohorts treated with AZD5991. Yet, at days 13-21, stable disease was only maintained in animals that received CAR-37 + AZD5991 (Fig. 6B). The combination of CAR-37 T cells and AZD5991 delayed tumor progression and significantly prolonged overall survival with an average of 41.3 days compared to 19.1 days in the CAR-37 T cell cohort and 33.4 days in the AZD5991 cohort (Fig. 6C). Importantly, these same results were achieved in a repeat experiment with two doses of AZD5991 administered weekly for three weeks (Figure S7A-C).

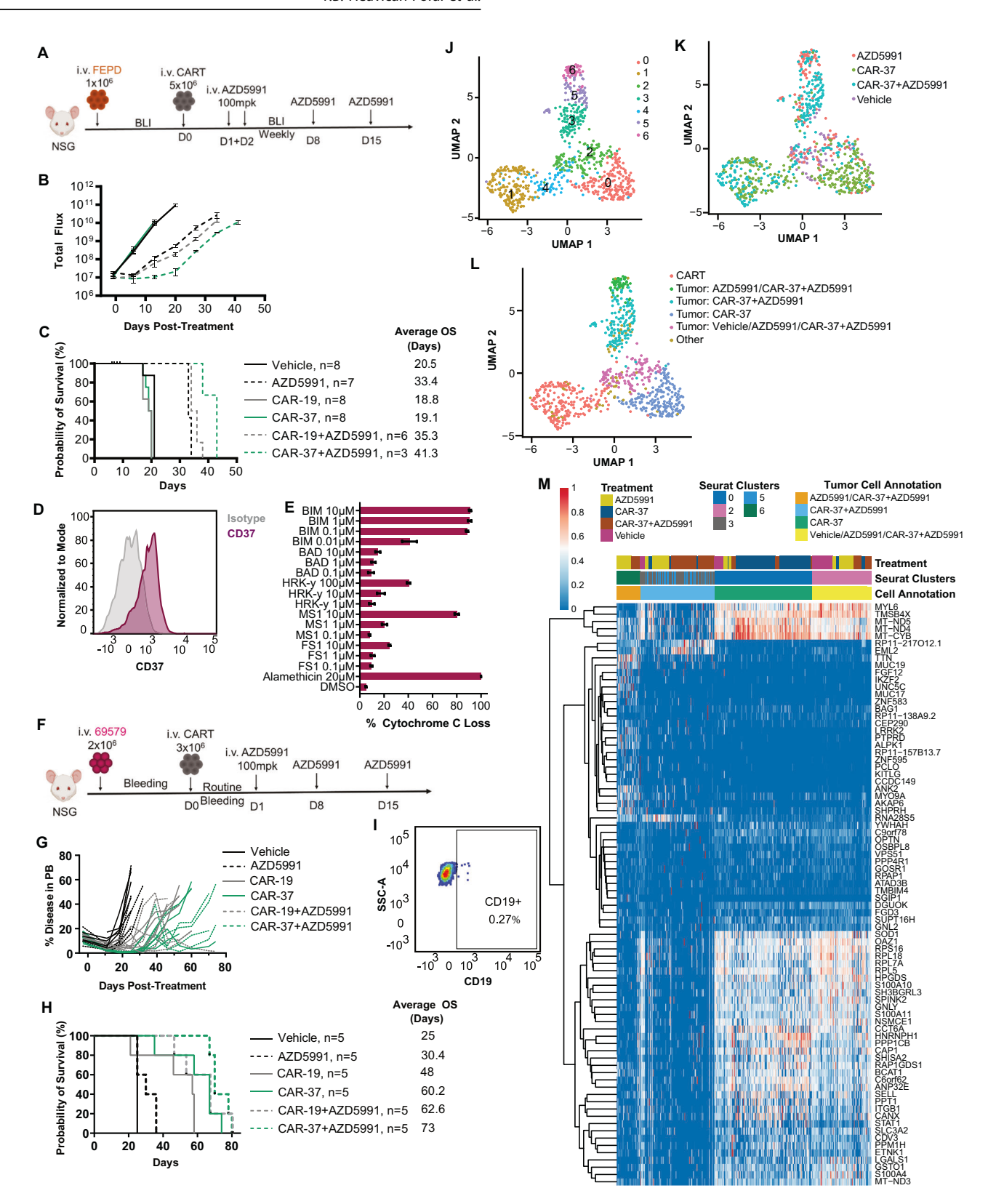
The same therapeutic combinations were evaluated against the CD37-postive, MCL-1 dependent adult T-cell leukemia/lymphoma (ATLL) PDX DFTL-69579 (Fig. 6D/E). Engraftment was monitored via peripheral blood and treatment started upon an average of 10% blood involvement (Fig. 6F). CAR-37 T-cell persistence was monitored at the same timepoints by flow cytometry and showed no difference when combined with AZD5991. Although not significant, the CAR-37 + AZD5991 cohort demonstrated an earlier CAR T-cell expansion at day 18 compared to the CAR-37 cohort at day 25 (Fig. S8A). We observed stably reduced tumor burden in all mice receiving AZD5991 while on treatment; however, immediate progression occurred in the AZD5991 cohort following the final dose. Progression was significantly delayed in the CAR-19 + AZD5991 and CAR-37 + AZD5991 cohorts leading to the longest overall survival with an average of 62.6 and 73 days, respectively (Fig. 6G/H). Notably, a small portion (<1%) of the tumor cells express CD19 (Fig. 6I) and may explain why the CAR-19 T cells alone and in combination with AZD5991 resulted in survival benefit.

To address antigen loss as a means of escape, we performed flow cytometry to determine CD37 antigen binding capacity on the surface of treated tumor cells harvested from the FEPD and DFTL-69579 mouse models (Fig. 6). As shown in Fig. S7D and Fig. S8B, there was no significant difference in antigen binding capacity between treatment cohorts, suggesting that resistance/ relapse was not due to CD37 antigen loss. Although not significant, there was a trend of increased CD37 antigen binding capacity on tumor cells from the CAR-37 + AZD5991 cohort in the DFTL-69579 model. Future work to focus on mechanisms of tumor relapse is warranted.

# Transcriptional profiling reveals tumor cell heterogeneity in response to therapeutic targeting with minimal effects on expanding CAR T cells

Transcriptional profiling was performed to evaluate the effect of AZD5991 on CAR-37 T cells in vivo and identify tumor cell response/resistance mechanisms. Splenic tumor and CAR-37 T cells from DFTL-69579-engrafted mice were collected on treatment day 14 (vehicle and CAR-37) or 15 (AZD5991 and CAR-37 + AZD5991) and subjected to SMART-seq2. Initial examination of transcriptional heterogeneity revealed seven clusters separated into three branches (Fig. 6J, Supplementary Table 1, Fig. S9A). Notably, one branch comprised of CAR-37 T cells from animals treated with CAR-37 T cells alone and in combination with AZD5991. Of the limited significant differential marker genes (n = 8) with a log2 fold-change  $\geq 1$ , all were more highly expressed in the CAR-37 T cells not exposed to AZD5991. Genes involved in T-cell activation and killing included SIT1, LCK, and GZMK. Functional phenotyping of CAR-37 T cells from the two conditions revealed similar expression levels of T-cell cytokine and proliferation signatures [40] (Fig. S9B, C). However, a significant increase in the T-cell cytotoxic signature [40] was detected in the CAR-37 T cells only cohort, which is largely driven by higher expression of GZMK and EOMES in these cells (Fig. S9D-F). Expression of activation markers CD69, IFNy, IL2RA, and OX40 was consistent between the two conditions as was expression of exhaustion markers PD-1, HAVCR2, TOX, and LAG3 (Fig. S9G-N). Next, more detailed CD8+T-cell phenotyping was performed and showed that expression of the four terminally exhausted T cell signatures was consistent between the two cohorts [41] (Fig. S9O-R)".

Thus, strong overlap of CAR-37 T cells from both conditions, combined with few differential marker genes and similar functional phenotypes, suggests that repeat AZD5991 exposure does not have a significant impact on expanding CAR-37 T cells (Fig. 6K).



The remaining two branches comprised of tumor cells distinguished by exposure to AZD5991 (Fig. 6K). Cell annotations were applied to group the CAR-37 T cells together and separate the tumor cells into four groups by treatments: 1) AZD5991 and CAR-37 + AZD5991, 2) CAR-37 + AZD5991, 3) CAR-37, and 4) a mix of primarily vehicle with some AZD5991 and CAR-37 + AZD5991.

The AZD5991 and CAR-37 + AZD5991 cells clustered with vehicle-treated cells likely represented cells that were not responding to treatment, and thus resistant. The cell type "other" refers to cells that clustered with the opposite cell type likely due to an impure sort and thus excluded from downstream analyses (Fig. 6L). The Molecular Signatures Database [42] was used to query the top 100

Fig. 6 Combining CAR-37 T cells and AZD5991 leads to enhanced targeting of MCL-1-dependent T-cell lymphoma in vivo. A Experiment schematic: NSG-DKO mice were injected intravenously with  $1 \times 10^6$  FEPD (CBG-GFP) cells and monitored by BLI for tumor burden weekly. Upon engraftment, mice were randomly assigned to 1 of 6 cohorts: vehicle, AZD5991, CAR-19, CAR-37, CAR-19 + AZD5991, or CAR-37 + AZD5591. On day 0,  $5 \times 10^6$  CAR-19 or CAR-37 T cells were administered to the respective treatment cohorts. Subsequently, mice in the AZD5991 cohorts received 100 mg/kg intravenously on days 1 and 2, 8, and 15 post-CAR T cells. B The average total flux (photons/seconds) of mice in the 6 treatment cohorts at weekly intervals. Mean ± SEM shown. C Kaplan-Meyer survival curve representing the survival trends of mice engrafted with FEPD and treated with vehicle, AZD5991, CAR-19, CAR-37, CAR-19 + AZD5991, or CAR-37 + AZD5991. Vehicle, CAR-19, and CAR-37; n = 8. AZD5991; n = 7. CAR-19 + AZD5991; n = 6. CAR-37 + AZD5991; n = 3. **D** Fluorescence-activated cell sorter (FACS) histograms of patient-derived xenograft line DFTL-69579 stained with CD37 and isotype control. **E** Mitochondrial apoptotic priming of DFTL-69579 cells measured by BH3 profiling. **F** Experiment schematic: NSG mice were injected intravenously with  $2 \times 10^6$  DFTL-69579 cells and monitored by blood engraftment. Upon engraftment, mice were randomly assigned to 1 of 6 cohorts: vehicle, AZD5991, CAR-19, CAR-37, CAR-19 + AZD5991, or CAR-37 + AZD5591. On day 0, 3×10<sup>6</sup> CAR-19 or CAR-37 T cells were administered to the respective treatment cohorts. Subsequently, mice in the AZD5991 cohorts received 100 mg/kg intravenously on days 1, 8, and 15 post-CAR T cells. G Disease monitoring in the peripheral blood of mice engrafted with DFTL-69579 via flow cytometry. H Kaplan-Meyer survival curve representing the survival trends of mice engrafted with DFTL-69579 and treated with vehicle, AZD5991, CAR-19, CAR-37, CAR-19 + AZD5991, or CAR-37 + AZD5991. n = 5. I FACS plot demonstrating a small percentage of DFTL-69579 neoplastic cells express CD19. J Uniform Manifold Approximation and Projection (UMAP) of the analyzed single cell RNA-seq data color-coded by defined Seurat clusters. K UMAP color-coded by treatment. L UMAP colorcoded by cell annotation manually defined based on clustering in (K). M Heatmap of the top 20 marker genes from each of the four tumor cell groups defined in (L).

marker genes (Supplementary Table 2) from the tumor cell groups, with the top 20 from each shown in Fig. 6M. Groups 1 and 2 consisting of AZD5991-treated tumor cells had low nCount (number of transcripts/cell) and nFeature (number of genes/cell) which is indicative of unhealthy, dying cells likely due to AZD5991 as cells were collected one hour after the final dose. A significant enrichment of gene signatures related to synapse, cell motility, and differentiation was detected in AZD5991 and CAR-37 + AZD5991-treated tumor cells. Surprisingly, there was a separate cluster of CAR-37 + AZD5991-treated tumor cells which were significantly enriched in signatures including FOXP3 bound/ target genes, which has been shown to be upregulated in a subset of ATLL [43, 44], and apoptosis via TRAIL, a known extrinsic apoptotic pathway induced by T cells likely induced by the CAR-37 T cells [45]. MYC target genes and MTORC1 signaling signatures were significantly enriched in tumor cells treated with only CAR-37 T cells. Lastly, group 4 which was predominately vehicle-treated tumor cells and presumed therapy-resistant cells from the single and combination treatment cohorts, was significantly enriched in MYC target and ribosomal/translation-related gene signatures which have been linked to therapy resistance [46, 47]. Notably, the same MYC signature (DANG BOUND BY MYC, M15774) was also enriched in cells treated with only CAR-37 T cells. MYC has been implicated in therapy resistance and CAR T cell resistance specifically [48, 49], thus warranting further investigation in TCL as a means of therapeutic escape.

### **DISCUSSION**

TCLs are associated with poor prognosis; thus, there is a significant need for improved therapeutic strategies. Immunotherapeutic approaches have been difficult to develop because TCLs often share phenotypic features of mature T cells. CD37 is a notable exception as it is almost exclusively expressed on malignant and not mature T cells. We demonstrated that CAR-37 T cells have strong anti-tumor activity against TCL via induction of apoptosis. However, akin to clinical response of aggressive B-cell lymphomas to CD19-directed CAR T cells [30, 31], response was not always durable. These observations highlight the need to potentiate CAR T-cell activity while maintaining tolerability. Using BH3 profiling to predict BH3 dependencies, we established the combination of CAR-37 T cells with the MCL-1 inhibitor AZD5991 as an effective treatment against TCL.

The identification of CD37 expression on TCL tumor cells and the absent/limited expression on non-malignant T cells makes CD37 a unique target compared to others (e.g., CD3, CD5, and CD7). Herein, we demonstrated CAR-37 T cells led to significant

killing of TCL cells and induced mitochondrial apoptosis. However, mitochondrial apoptosis is likely not the only mechanism of CARmediated killing [50]. As such, it was recently reported that knockout of Bak and Bax in B-cell lymphoma lines did not confer CAR-19 T-cell resistance, which it did in solid tumor models [33]. Along similar lines and as expected, we demonstrated that MCL-1 sensitivity was not dependent on CD37 expression in a WT and CD37-transduced T-cell lymphoma cell line (SMZ1) by demonstrating similar response curves to AZD5991 (Fig. S10). This suggests that CD37-negative antigen escape mutants would still be targeted by the MCL-1 inhibitor and supports the idea that by combining CAR T cells and BH3 mimetics tumor cells would need to establish two separate mechanisms of resistance. Additionally, our responses were observed in an antigen binding capacitydriven manner that was heightened by increasing effector to target cell ratios as others have seen [51-53]. These findings suggest that CAR T-cell treatment increases TCL susceptibility to apoptotic inhibitors, and thus provide rationale for evaluating such combinations as done against other hematological maliqnancies with T and NK-based immunotherapies [27-29].

Previous efforts revealed MCL-1 as the most expressed and functionally dependent antiapoptotic BCL-2 family member in TCL (>50%) [20]. Herein, our results confirmed those findings and demonstrated that the selective MCL-1 inhibitor AZD5991 [23], was the most potent BH3 mimetic against the CD37-positive TCL lines DL-40, FEPD, MTA, and SMZ1 + CD37 [20]. Of note, a recent phase 1 clinical trial with AZD5991 faced challenges of reduced drug efficacy and dose limiting toxicities, including cardiac toxicity [54]. However, the combination of AZD5991 with CAR T cells increases the possibility of a shorter AZD5991-treatment duration and therefore could avoid potential toxicities. Although further investigation would be needed, it is useful to have drug combinations in cellular immunotherapy regimens such as those presented here, where one drug can be titrated or dosed daily and see reversible effects. Additionally, we recommend performing BH3 profiling on each tumor to define the specific apoptotic dependence/s and maximize targeting for a personalized approach. Before combining BH3 mimetics and CAR-37 T cells, two critical factors needed addressed—both antigen binding capacity on the target cells and CAR T-cell function/viability needed to be maintained in the presence of BH3 mimetics. Indeed, antigen binding capacity was not reduced and, CAR T-cell viability remained greater than 85% in all conditions with no changes in immunophenotype distribution and expression of T-cell activation/exhaustion markers, both of which have critical roles in effective CAR T-cell antitumor activity [55]. Interestingly, BH3 profiling predicted CAR T cells to be dependent on BCL-xL,

which was heightened when stimulated with target cells. Prior data suggest expanding T cells upregulate BCL-xL to avoid activation-induced cell death [56-58], and we observed elevated cytochrome c release in response the BCL-2/BCL-xL inhibitor ABT263 (Fig. S11). Thus, with the potential negative impact of ABT263 on CAR-37 T cells and the known effects it has on platelets in vivo [59], future studies exploring alternative BCL-xL inhibitors and/or methods to evade potential dependence on BCL-xL are warranted. In a similar effort, we recently reported that overexpression of BCL-xL in CAR-19 T cells resulted in improved persistence and function with greater tolerance to BH3 mimetics [60]. Additionally, when evaluating higher concentrations of the BH3 mimetics (Fig. 3D), IL-2 stimulated CAR T cells derived from two donors were sensitive to AZD5991. Therefore, there is importance in profiling CAR T cells prior to combination with BH3 mimetics. Fortunately, the AZD5991-senstive donor cells maintained ≥50% viability at a concentration effective to target the MCL1-dependent lines in vitro, and sensitivity was substantially lessened when stimulated with target tumor cells rather than IL-2, suggesting activation may lower dependence. Thus, we noted high variability of both lymphoma and normal T cells to MCL-1 inhibition. Future studies will need to use larger data sets to examine the frequency of MCL-1 inhibition in both sets of cells. For clinical implementation, we recommend BH3 profiling of T cells prior to CAR T-cell manufacturing. This would require a blood draw prior to apheresis collection. To test the tumor cells, we would recommend obtaining a hollow core needle biopsy, which would provide 50-200,000 cells. This provides sufficient cells to assess MCL-1 dependence in the tumor cells, and it is standard practice for clinicians to obtain a biopsy at relapse. We would then recommend restricting the addition of the MCL-1 inhibitor to those patients whose T cells were less MCL-1 dependent than their tumor cells.

In our study, combining CAR-37 T cells with AZD5991 resulted in significantly improved tumor cell killing in MCL-1-dependent/ CD37-positive TCLs. We considered that it was possible that AZD5991 enhanced the susceptibility of tumor cells to T-cell killing more broadly, and independent of the CAR antigen (Fig. S6A-C). This would not be expected to occur with autologous T cell therapies, but theoretically, AZD5991 could also enhance the cytotoxic effects of allogeneic T-cell products or other immunotherapies. We acknowledge that based on the current study, the benefit of this combination in an autologous setting is unclear. With this noted limitation, we would suggest future CAR T cell and small molecule combination studies to explore alloreactivity effects using CD3 knockout T cells or tumor models engineered with MHC I/II knockout. Additionally, other groups have evaluated the effects of combining BH3 mimetics (e.g., ABT199, S63845, and ABT737) with CAR-19 T cells against CD19positive malignancies [28, 29]. Although under some circumstances CAR-19 T cell quantity was reduced by exposure to the BH3 mimetics, the quality of the T-cell response was enhanced, particularly in the CD8-positive CAR T-cell population [29]. Corresponding to our results, both studies observed that dosing treshe BH3 mimetics prior to or simultaneously with the CAR-19 T cells improved tumor cell killing compared to either treatment alone [28, 29]. Yet, one group reported the greatest effect was achieved when the tumor cells were pre-sensitized with the BH3 mimetic. The authors acknowledged this result may be due to increased target antigen expression following BH3 mimetic treatment as observed in one of their models [29]. However, this was not a consistent trend observed on our tumor cells following BH3 mimetic exposure. Determining if pre-, simultaneous, or posttreatment of BH3 mimetics with CAR T cells is optimal may depend on individual donor T cell sensitivities and warrants further investigation in the setting of TCL and with constructs other than CAR-19.

Notably, not all TCL lines or PDXs screened expressed CD37. Given the lack of effective treatments for TCLs we would argue that further clinical development of combination therapies will need to incorporate clinical diagnostic screening for BH3 dependence and immunotherapeutic target expression to tailor combination strategies for those patients who might benefit the most. Additionally, through the course of a phase 1 clinical trial [61], CAR-37 T-cells had strong anti-tumor activity, but clinical benefit was ultimately limited due to both prolonged inflammation and CD37 antigen loss. It is not clear if MCL-1 inhibition would reduce these particular toxicities, but the combination may enable improved eradication of disease, as we demonstrate herein, in conjunction with toxicity-mitigation strategies such as use of lower doses or blockade of other cytokines, such as IFNy or IL-18, as observed in vitro in Fig. S4.

In summary, there is a significant need for improved therapeutics for patients with TCL. Our results provide preclinical evidence that combining CAR-37 T cells and selective BH3 mimetics improves TCL targeting by pushing the tumor cells over their apoptotic threshold. Not only could these results be used to nominate and/or deprioritize future combination strategies for patients with TCL, but also for patients being treated with effector T cells for a range of hematologic malignancies.

### **DATA AVAILABILITY**

The SMART-Seq2 data is available under GSE287873.

### **REFERENCES**

- Vose J, Armitage J, Weisenburger D, International TCLP. International peripheral T-cell and natural killer/T-cell lymphoma study: pathology findings and clinical outcomes. J Clin Oncol. 2008;26:4124–30.
- Alaggio R, Amador C, Anagnostopoulos I, Attygalle AD, Araujo IBO, Berti E, et al. The 5th edition of the World Health Organization classification of haematolymphoid tumours: lymphoid neoplasms. Leukemia. 2022;36:1720–48.
- Moskowitz AJ, Lunning MA, Horwitz SM. How I treat the peripheral T-cell lymphomas. Blood. 2014:123:2636–44.
- Wilcox RA. Optimising initial treatment for peripheral T-cell lymphoma: a tough nut to CHOP. Lancet Haematol. 2018;5:e182–e3.
- 5. Zhang Q, Wang S, Chen J, Yu Z. Histone deacetylases (HDACs) guided novel therapies for T-cell lymphomas. Int J Med Sci. 2019;16:424–42.
- O'Connor OA, Pro B, Pinter-Brown L, Bartlett N, Popplewell L, Coiffier B, et al. Pralatrexate in patients with relapsed or refractory peripheral T-cell lymphoma: results from the pivotal PROPEL study. J Clin Oncol. 2011;29:1182–9.
- Zinzani PL, Musuraca G, Tani M, Stefoni V, Marchi E, Fina M, et al. Phase II trial of proteasome inhibitor bortezomib in patients with relapsed or refractory cutaneous T-cell lymphoma. J Clin Oncol. 2007;25:4293–7.
- Abramson JS. Anti-CD19 CAR T-cell therapy for B-cell non-hodgkin lymphoma. Transfus Med Rev. 2020;34:29–33.
- Ma G, Wang Y, Ahmed T, Zaslav AL, Hogan L, Avila C, et al. Anti-CD19 chimeric antigen receptor targeting of CD19+acute myeloid leukemia. Leuk Res Rep. 2018:9:42-4.
- Safarzadeh Kozani P, Safarzadeh Kozani P, Rahbarizadeh F. CAR-T cell therapy in T-cell malignancies: Is success a low-hanging fruit. Stem Cell Res Ther. 2021;12:527.
- Cooper ML, Choi J, Staser K, Ritchey JK, Devenport JM, Eckardt K, et al. An "offthe-shelf" fratricide-resistant CAR-T for the treatment of T cell hematologic malignancies. Leukemia. 2018;32:1970–83.
- Gomes-Silva D, Srinivasan M, Sharma S, Lee CM, Wagner DL, Davis TH, et al. CD7edited T cells expressing a CD7-specific CAR for the therapy of T-cell malignancies. Blood. 2017;130:285–96.
- Maciocia PM, Wawrzyniecka PA, Philip B, Ricciardelli I, Akarca AU, Onuoha SC, et al. Targeting the T cell receptor beta-chain constant region for immunotherapy of T cell malignancies. Nat Med. 2017;23:1416–23.
- Mamonkin M, Mukherjee M, Srinivasan M, Sharma S, Gomes-Silva D, Mo F, et al. Reversible transgene expression reduces fratricide and permits 4-1BB costimulation of CAR T cells directed to T-cell malignancies. Cancer Immunol Res. 2018;6:47–58.
- Mamonkin M, Rouce RH, Tashiro H, Brenner MK. A T-cell-directed chimeric antigen receptor for the selective treatment of T-cell malignancies. Blood. 2015;126:983–92.

- Png YT, Vinanica N, Kamiya T, Shimasaki N, Coustan-Smith E, Campana D. Blockade of CD7 expression in T cells for effective chimeric antigen receptor targeting of T-cell malignancies. Blood Adv. 2017;1:2348–60.
- 17. Mulvey E, Ruan J. Biomarker-driven management strategies for peripheral T cell lymphoma. J Hematol Oncol. 2020;13:59.
- Went P, Agostinelli C, Gallamini A, Piccaluga PP, Ascani S, Sabattini E, et al. Marker expression in peripheral T-cell lymphoma: a proposed clinical-pathologic prognostic score. J Clin Oncol. 2006;24:2472–9.
- Scarfo I, Ormhoj M, Frigault MJ, Castano AP, Lorrey S, Bouffard AA, et al. Anti-CD37 chimeric antigen receptor T cells are active against B- and T-cell lymphomas. Blood. 2018;132:1495–506.
- Koch R, Christie AL, Crombie JL, Palmer AC, Plana D, Shigemori K, et al. Biomarkerdriven strategy for MCL1 inhibition in T-cell lymphomas. Blood. 2019;133:566–75.
- Souers AJ, Leverson JD, Boghaert ER, Ackler SL, Catron ND, Chen J, et al. ABT-199, a potent and selective BCL-2 inhibitor, achieves antitumor activity while sparing platelets. Nat Med. 2013;19:202–8.
- 22. Tse C, Shoemaker AR, Adickes J, Anderson MG, Chen J, Jin S, et al. ABT-263: a potent and orally bioavailable Bcl-2 family inhibitor. Cancer Res. 2008;68:3421–8.
- Tron AE, Belmonte MA, Adam A, Aquila BM, Boise LH, Chiarparin E, et al. Discovery of Mcl-1-specific inhibitor AZD5991 and preclinical activity in multiple myeloma and acute myeloid leukemia. Nat Commun. 2018;9:5341.
- Montero J, Letai A. Dynamic BH3 profiling-poking cancer cells with a stick. Mol Cell Oncol. 2016;3:e1040144.
- Ryan J, Montero J, Rocco J, Letai A. iBH3: simple, fixable BH3 profiling to determine apoptotic priming in primary tissue by flow cytometry. Biol Chem. 2016;397:671–8
- 26. Cidado J, Boiko S, Proia T, Ferguson D, Criscione SW, San Martin M, et al. AZD4573 is a highly selective CDK9 inhibitor that suppresses MCL-1 and induces apoptosis in hematologic cancer cells. Clin Cancer Res. 2020;26:922–34.
- Pan R, Ryan J, Pan D, Wucherpfennig KW, Letai A. Augmenting NK cell-based immunotherapy by targeting mitochondrial apoptosis. Cell. 2022;185:1521–38
- 28. Karlsson H, Lindqvist AC, Fransson M, Paul-Wetterberg G, Nilsson B, Essand M, et al. Combining CAR T cells and the Bcl-2 family apoptosis inhibitor ABT-737 for treating B-cell malignancy. Cancer Gene Ther. 2013;20:386–93.
- Yang M, Wang L, Ni M, Neuber B, Wang S, Gong W, et al. Pre-sensitization of malignant B cells through venetoclax significantly improves the cytotoxic efficacy of CD19.CAR-T cells. Front Immunol. 2020;11.
- 30. Xu X, Sun Q, Liang X, Chen Z, Zhang X, Zhou X, et al. Mechanisms of relapse after CD19 CAR T-cell therapy for acute lymphoblastic leukemia and its prevention and treatment strategies. Front Immunol. 2019;10:2664.
- Hunter BD, Rogalski M, Jacobson CA. Chimeric antigen receptor T-cell therapy for the treatment of aggressive B-cell non-Hodgkin lymphomas: efficacy, toxicity, and comparative chimeric antigen receptor products. Expert Opin Biol Ther. 2019:19:1157–64.
- 32. Messmer MN, Snyder AG, Oberst A. Comparing the effects of different cell death programs in tumor progression and immunotherapy. Cell Death Differ. 2019;26:115–29.
- Pourzia A, Olson M, Bailey S, Aryal A, Ryan J, Maus M, et al. 269 Mitochondrial apoptosis mediates CAR T cell cytotoxicity. J Immunother Cancer. 2022:10:A284–A.
- 34. Yan X, Chen D, Wang Y, Guo Y, Tong C, Wei J, et al. Identification of NOXA as a pivotal regulator of resistance to CAR T-cell therapy in B-cell malignancies. Signal Transduct Target Ther. 2022;7:98.
- 35. Nam KO, Shin SM, Lee HW. Cross-linking of 4-1BB up-regulates IL-13 expression in CD8(+) T lymphocytes. Cytokine. 2006;33:87–94.
- Shin SM, Kim YH, Choi BK, Kwon PM, Lee HW, Kwon BS. 4-1BB triggers IL-13 production from T cells to limit the polarized, Th1-mediated inflammation. J Leukoc Biol. 2007;81:1455–65.
- Certo M, Del Gaizo Moore V, Nishino M, Wei G, Korsmeyer S, Armstrong SA, et al. Mitochondria primed by death signals determine cellular addiction to antiapoptotic BCL-2 family members. Cancer Cell. 2006:9:351–65.
- Chen L, Willis SN, Wei A, Smith BJ, Fletcher JI, Hinds MG, et al. Differential targeting of prosurvival Bcl-2 proteins by their BH3-only ligands allows complementary apoptotic function. Mol Cell. 2005;17:393–403.
- Kuwana T, Bouchier-Hayes L, Chipuk JE, Bonzon C, Sullivan BA, Green DR, et al. BH3 domains of BH3-only proteins differentially regulate Bax-mediated mitochondrial membrane permeabilization both directly and indirectly. Mol Cell. 2005;17:525–35.
- Szabo PA, Levitin HM, Miron M, Snyder ME, Senda T, Yuan J, et al. Single-cell transcriptomics of human T cells reveals tissue and activation signatures in health and disease. Nat Commun. 2019;10:4706.
- 41. Zheng L, Qin S, Si W, Wang A, Xing B, Gao R, et al. Pan-cancer single-cell landscape of tumor-infiltrating T cells. Science. 2021;374:abe6474.

- Subramanian A, Tamayo P, Mootha VK, Mukherjee S, Ebert BL, Gillette MA, et al. Gene set enrichment analysis: a knowledge-based approach for interpreting genome-wide expression profiles. Proc Natl Acad Sci USA. 2005;102:15545–50.
- Karube K, Aoki R, Sugita Y, Yoshida S, Nomura Y, Shimizu K, et al. The relationship of FOXP3 expression and clinicopathological characteristics in adult T-cell leukemia/lymphoma. Mod Pathol. 2008;21:617–25.
- Roncador G, Garcia JF, Garcia JF, Maestre L, Lucas E, Menarguez J, et al. FOXP3, a selective marker for a subset of adult T-cell leukaemia/lymphoma. Leukemia. 2005;19:2247–53.
- 45. Lee YG, Yang N, Chun I, Porazzi P, Carturan A, Paruzzo L, et al. Apoptosis: a Janus bifrons in T-cell immunotherapy. J Immunother Cancer. 2023;11.
- Elhamamsy AR, Metge BJ, Alsheikh HA, Shevde LA, Samant RS. Ribosome biogenesis: a central player in cancer metastasis and therapeutic resistance. Cancer Res. 2022:82:2344–53.
- 47. Donati G, Amati B. MYC and therapy resistance in cancer: risks and opportunities. Mol Oncol. 2022;16:3828–54.
- Yan F, Jiang V, Jordan A, Che Y, Liu Y, Cai Q, et al. The HSP90-MYC-CDK9 network drives therapeutic resistance in mantle cell lymphoma. Exp Hematol Oncol. 2024;13:14.
- Sworder BJ, Kurtz DM, Alig SK, Frank MJ, Shukla N, Garofalo A, et al. Determinants of resistance to engineered T cell therapies targeting CD19 in large B cell lymphomas. Cancer Cell. 2023;41:210–25 e5.
- Benmebarek MR, Karches CH, Cadilha BL, Lesch S, Endres S, Kobold S Killing Mechanisms of chimeric antigen receptor (CAR) T cells. Int J Mol Sci. 2019;20.
- Walker AJ, Majzner RG, Zhang L, Wanhainen K, Long AH, Nguyen SM, et al. Tumor antigen and receptor densities regulate efficacy of a chimeric antigen receptor targeting anaplastic lymphoma kinase. Mol Ther. 2017;25:2189–201.
- Watanabe K, Terakura S, Martens AC, van Meerten T, Uchiyama S, Imai M, et al. Target antigen density governs the efficacy of anti-CD20-CD28-CD3 zeta chimeric antigen receptor-modified effector CD8+ T cells. J Immunol. 2015;194:911–20.
- Majzner RG, Mackall CL. Tumor antigen escape from CAR T-cell therapy. Cancer Discov. 2018;8:1219–26.
- 54. Desai P, Lonial S, Cashen A, Kamdar M, Flinn I, O'Brien S, et al. A phase 1 first-in-human study of the MCL-1 inhibitor AZD5991 in patients with relapsed/refractory hematologic malignancies. Clin Cancer Res. 2024;30:4844–55.
- Fraietta JA, Lacey SF, Orlando EJ, Pruteanu-Malinici I, Gohil M, Lundh S, et al. Determinants of response and resistance to CD19 chimeric antigen receptor (CAR) T cell therapy of chronic lymphocytic leukemia. Nat Med. 2018;24:563–71.
- Guerrero AD, Welschhans RL, Chen M, Wang J. Cleavage of anti-apoptotic Bcl-2 family members after TCR stimulation contributes to the decision between T cell activation and apoptosis. J Immunol. 2013;190:168–73.
- Lee HW, Park SJ, Choi BK, Kim HH, Nam KO, Kwon BS. 4-1BB promotes the survival of CD8+ T lymphocytes by increasing expression of Bcl-xL and Bfl-1. J Immunol. 2002;169:4882–8.
- Maus MV, Thomas AK, Leonard DG, Allman D, Addya K, Schlienger K, et al. Ex vivo expansion of polyclonal and antigen-specific cytotoxic T lymphocytes by artificial APCs expressing ligands for the T-cell receptor, CD28 and 4-1BB. Nat Biotechnol. 2002;20:143–8.
- Kaefer A, Yang J, Noertersheuser P, Mensing S, Humerickhouse R, Awni W, et al. Mechanism-based pharmacokinetic/pharmacodynamic meta-analysis of navitoclax (ABT-263) induced thrombocytopenia. Cancer Chemother Pharm. 2014;74:593–602.
- Korell F, Olson ML, Salas-Benito D, Leick MB, Larson RC, Bouffard A, et al. Comparative analysis of Bcl-2 family protein overexpression in CAR T cells alone and in combination with BH3 mimetics. Sci Transl Med. 2024;16:eadk7640.
- Frigault MJ, Graham CE, Berger TR, Ritchey J, Horick NK, El-Jawahri A, et al. Phase 1 study of CAR-37 T cells in patients with relapsed or refractory CD37+ lymphoid malignancies. Blood. 2024;144:1153–67.

### **ACKNOWLEDGEMENTS**

We thank the Flow Cytometry Core, Molecular Diagnostics Core, and Animal Research Facility at Dana-Farber Cancer Institute for their assistance. AZD5991 was kindly provided by AstraZeneca. The graphical abstract and the mouse graphics were created with BioRender. This work was supported by NCI P01 CA233412 (DMW, MVM, and BK). TBH receives funding from the Lymphoma Research Foundation and Helen Gurley Brown Presidential Initiative at Dana-Farber Cancer Institute. FK receives funding by the German Research Foundation (DFG; 466535590). GW is Fellow of The Leukemia & Lymphoma Society. KS is supported by NIH R35 CA210030. DMW was supported by NCI R35 CA231958 and Leukemia and Lymphoma Society Specialized Center of Research 7026-21. MVM is supported by NIH CA249062.

### 2464

### **AUTHOR CONTRIBUTIONS**

All authors have either conceived, acquired, and/or interpreted the results. Additionally, all authors have revised the manuscript, approved the final version, and agreed to be accountable for all aspects of the work. Specifically, TBH, IS, AL, KS, JL, DMW, MVM, and BK conceptualized this study and interpreted results. TBH, FK, IS, CW, AB, ZE, FP, JH, JL, SK, HS, and GW executed and analyzed the experiments. TBH and BK co-wrote the manuscript which was revised and approved by all authors.

#### **FUNDING**

This work was supported by NCI P01 CA233412 (DMW, MVM, and BK). TBH receives funding from the Lymphoma Research Foundation and Helen Gurley Brown Presidential Initiative at Dana-Farber Cancer Institute. FK receives funding by the German Research Foundation (DFG; 466535590). GW is Fellow of The Leukemia & Lymphoma Society. KS is supported by NIH R35 CA210030. DMW was supported by NCI R35 CA231958 and Leukemia and Lymphoma Society Specialized Center of Research 7026-21. AL and MVM are supported by NIH CA249062.

### **COMPETING INTERESTS**

IS is an employee of ArsenalBio. AL is on the Scientific Advisory Boards of Zentalis Pharmaceuticals and Flash Therapeutics. KS is on the SAB and has stock options in Auron Therapeutics. KS receives grant funding from Novartis and KronosBio on topics unrelated to this manuscript. JGL received research funding from Bristol Myers Squibb for an unrelated project. DMW received research support from Daiichi Sankyo, AstraZeneca, Abcuro, and Secura for unrelated projects and is now an employee of Merck/MSD. M.V.M. has received research support from Kite Pharma, Servier, and Novartis for unrelated projects, is a member of the Board of Directors of 2SeventyBio, and has served as a consultant for WindMIL, Tmunity, TCR2, Sanofi, Novartis, Neximmune, Micromedicine/BendBio, Kite Pharma, Intellia, In8bio, CRISPR Therapeutics, Cabaletta Bio, BMS, Bayer, AzstraZeneca, Astellas, Arcellx, Adaptimmune, Agenus, and Allogene; none of these are related to the work herein. AZD5991 was provided by AstraZeneca. The other authors declared no relevant conflicts of interest.

### ETHICS APPROVAL AND CONSENT TO PARTICIPATE

All methods were performed in accordance with the relevant guidelines and regulations. Vertebrate animal work was performed according to Dana-Farber Cancer

Institute's IACUC-approved protocol #13–034 or Massachusetts General Hospital's IACUC-approved protocol #2020N000114.

### **ADDITIONAL INFORMATION**

**Supplementary information** The online version contains supplementary material available at https://doi.org/10.1038/s41375-025-02697-1.

**Correspondence** and requests for materials should be addressed to Marcela V. Maus or Birgit Knoechel.

Reprints and permission information is available at http://www.nature.com/

**Publisher's note** Springer Nature remains neutral with regard to jurisdictional claims in published maps and institutional affiliations.

<u>@⊕</u>\$≘

**Open Access** This article is licensed under a Creative Commons Attribution-NonCommercial-NoDerivatives 4.0 International License.

which permits any non-commercial use, sharing, distribution and reproduction in any medium or format, as long as you give appropriate credit to the original author(s) and the source, provide a link to the Creative Commons licence, and indicate if you modified the licensed material. You do not have permission under this licence to share adapted material derived from this article or parts of it. The images or other third party material in this article are included in the article's Creative Commons licence, unless indicated otherwise in a credit line to the material. If material is not included in the article's Creative Commons licence and your intended use is not permitted by statutory regulation or exceeds the permitted use, you will need to obtain permission directly from the copyright holder. To view a copy of this licence, visit <a href="http://creativecommons.org/licenses/by-nc-nd/4.0/">http://creativecommons.org/licenses/by-nc-nd/4.0/</a>.

© The Author(s) 2025